Received: 29 November 2022 | Revised: 15 February 2023 | Accepted: 15 February 2023

DOI: 10.1111/epi.17551

Epilepsia®

RESEARCH ARTICLE

Altered spreading of neuronal avalanches in temporal lobe epilepsy relates to cognitive performance: A resting-state hdEEG study

Gian Marco Duma[1] | **Alberto Danieli**[1] | **Giovanni Mento**[2,3] | **Valerio Vitale**[4] | **Raffaella Scotto Opipari**[4] | **Viktor Jirsa**[5] | **Paolo Bonanni**[1] | **Pierpaolo Sorrentino**[5]

[1]Epilepsy Unit, IRCCS E. Medea Scientific Institute, Treviso, Italy

[2]Department of General Psychology, University of Padova, Padova, Italy

[3]Padova Neuroscience Center (PNC), University of Padova, Padova, Italy

[4]Department of Neuroscience, Neuroradiology Unit, San Bortolo Hospital, Vicenza, Italy

[5]Institut de Neurosciences des Systèmes, Aix-Marseille Université, Marseille, France

Correspondence
Gian Marco Duma, Epilepsy Unit, IRCCS E. Medea Scientific Institute, Via Costa Alta 37, Conegliano, Treviso 31015, Italy.
Email: gianmarco.duma@lanostrafamiglia.it

Funding information
Ministero della Salute, Grant/Award Number: 5 x mille; European Union's Horizon 2020, Grant/Award Number: 945539 (SGA3)

Abstract

Objective: Large aperiodic bursts of activations named neuronal avalanches have been used to characterize whole-brain activity, as their presence typically relates to optimal dynamics. Epilepsy is characterized by alterations in large-scale brain network dynamics. Here we exploited neuronal avalanches to characterize differences in electroencephalography (EEG) basal activity, free from seizures and/or interictal spikes, between patients with temporal lobe epilepsy (TLE) and matched controls.

Method: We defined neuronal avalanches as starting when the *z*-scored source-reconstructed EEG signals crossed a specific threshold in any region and ending when all regions returned to baseline. This technique avoids data manipulation or assumptions of signal stationarity, focusing on the aperiodic, scale-free components of the signals. We computed individual avalanche transition matrices to track the probability of avalanche spreading across any two regions, compared them between patients and controls, and related them to memory performance in patients.

Results: We observed a robust topography of significant edges clustering in regions functionally and structurally relevant for the TLE, such as the entorhinal cortex, the inferior parietal and fusiform area, the inferior temporal gyrus, and the anterior cingulate cortex. We detected a significant correlation between the centrality of the entorhinal cortex in the transition matrix and the long-term memory performance (delay recall Rey–Osterrieth Complex Figure Test).

Significance: Our results show that the propagation patterns of large-scale neuronal avalanches are altered in TLE during the resting state, suggesting a potential diagnostic application in epilepsy. Furthermore, the relationship between specific patterns of propagation and memory performance support the neurophysiological relevance of neuronal avalanches.

KEYWORDS

EEG source imaging, memory, neuronal avalanches, resting state, temporal lobe epilepsy

1 | INTRODUCTION

Empirical evidence supports the hypothesis that the human brain displays near critical dynamics, characterized by the coexistence of large, aperiodic bursts of activations ("neuronal avalanches") and oscillatory activity.[1] The scale-invariant properties shown by brain signals have been associated with a dynamical regimen supporting maximally efficient and flexible information processing.[2]

Epilepsy is a neurological disorder characterized by recurrent, unprovoked seizures, the generation and propagation of which depend on the activation of networks of interrelated brain regions, defined as an "epileptogenic network" (EN).[3]

According to its first, mainly empirical conceptualization, which arose in the context of stereo-electroencephalographic presurgical assessment of focal epilepsy, the EN represents the set of brain regions involved in the primary organization of an individual's ictal discharge, and the ultimate target of surgical treatment.[4] From a broader perspective, network theory is applied in the context of epilepsy as a framework to describe, with different methodologies, the complex spatiotemporal organization of the EN activity (ictal and interictal),[5–7] as well as its overall clinical impact, which may include cognitive dysfunction.[8]

The critical brain hypothesis may provide a further and complementary framework to describe complex brain network dynamics, with important applications for the study of neurological disorders.[9] In particular, large aperiodic bursts of activations that spread across the brain (named "neuronal avalanches") have been observed in large-scale neurophysiological recordings.[10] More recently, avalanche transition matrices have been applied to magneto/electroencephalography (M/EEG) data, in order to encapsulate the spatiotemporal spreading of neuronal avalanches on a large scale. These studies highlighted that neuronal avalanches spread preferentially across the white-matter bundles,[11,12] and that they are drastically altered in neurodegenerative diseases.[11–13] In the context of epilepsy, the criticality framework has been used to investigate global brain dynamics during ictal and interictal epileptic activity,[14–16] showing a deviation of the system from the critical state in both conditions.

In recent years, a significant body of research has investigated the intrinsic functional organization of brain dynamics in the resting-state (RS) condition. Notably, epilepsy-related cognitive abnormalities have been linked to an altered architecture of functional brain networks at rest.[8,17] Most of these approaches are based on the analysis of the covariation between the corresponding signals and/or spectral power, as well as the frequency-specific phase locking (i.e. synchronization). However, such techniques rely on the assumption of stationarity. In the present work, we investigated neuronal avalanche dynamics during RS in patients with temporal lobe epilepsy (TLE). We hypothesized that even during RS the spatial spreading of neuronal avalanches would display specific alterations in individuals with TLE compared to controls. More precisely, we predicted that large-scale neuronal avalanches, as they spread across the brain at rest, would more likely recruit regions that are known to be functionally relevant for seizure generation and propagation in TLE. Moreover, we hypothesized that abnormalities of neuronal avalanche dynamics in TLE would be associated with neuropsychological performances, which are typically altered in patients with TLE. To test these hypotheses, we estimated the neuronal avalanche transition matrices from source-reconstructed EEG acquired in patients with TLE and matched healthy controls. From the resting activity, we estimated the probability of a neuronal avalanche spreading between any pair of brain regions. Comparing (edge-wise) these probabilities in the two groups allowed us to identify, in an unsupervised, data-driven fashion, the regions that displayed altered aperiodic dynamics in individuals with TLE compared to controls. Finally, we related the altered recruitment of such regions to cognitive performance.

Key Points

- Investigation of the brain dynamics during resting-state activity in patients with temporal lobe epilepsy (TLE) using neuronal avalanches (i.e., large-scale patterns of activation)
- We found higher transition probabilities in patients with TLE in the entorhinal cortex, inferior temporal and fusiform gyri, and anterior cingulate cortex
- We found higher eigenvector centrality of the left entorhinal cortex in the avalanche transition matrix, which was related to reduced long-term memory performance
- Discussion of the potential application of the avalanche transition matrix as a diagnostic tool in presurgical evaluations and epilepsy type differentiation

2 | METHOD

2.1 | Participants

Between January 2018 and December 2020 a total of 49 patients with drug-resistant TLE underwent high-density

EEG (hdEEG) recording as part of the presurgical evaluation at IRCCS E. Medea, Conegliano (Treviso), Italy. The presurgical workup included detailed clinical history and examination, neuropsychological assessment, long-term surface video-EEG monitoring, and 3 T brain magnetic resonance imaging (MRI), with positron emission tomography (PET) as an adjunctive investigation in select cases. The sample size was determined based on the subject availability of the clinical center. The inclusion criteria were: - age ≥18 years; – temporal seizure onset based on clinical history and ictal video-EEG recordings; – MRI evidence of epileptogenic lesion confined to the temporal lobe or negative MRI; – RS activity recorded with hdEEG ≥8 min. A total of 37 patients, 16 left TLE, 8 right TLE, 13 bitemporal, (mean age = 46.73 [SD = 15.18]; 20 female) were eligible for the study.

The mean number of antiseizure medications (ASMs) per person was equal to 2.05 with a range from a minimum of 0 to a maximum of 5 ASMs. Specifically, among the patients with TLE, three had no medication, nine had monotherapy, and the rest of participants had polytherapy. A description of patients' demographic and clinical characteristics is given in Table 1.

The control group was composed of 35 healthy participants with no history of neurological or psychiatric disorders (mean age = 35.10 [SD = 8.24]; 28 female). The study was conducted according to the principles expressed in the Declaration of Helsinki and approved by the local ethical committee.

2.2 | Neuropsychological scores

All the patients with TLE underwent a neuropsychological evaluation focusing on memory, attention/executive functions, and intelligence. Specifically, long-term non-verbal and verbal memory was investigated with the delay recall of the Rey–Osterrieth Complex Figure Test (ROCFT)[18] and the Rey Auditory Verbal Learning Test (RAVLT).[19] Attention and executive functions were evaluated with the Trail Making Test (TMT).[20] Specifically, we included in the analysis both the part A and B as a measure of motor speed and attention shifting capabilities, respectively. Finally, we used the total IQ (TIQ) of the WAIS-IV scale[21] as a global intelligence measure. However, not all patients completed the assessment. Therefore, we reduced the sample size to 27 patients for the analyses of the correlation of the neuropsychological functioning with the neural activity. Summary statistics for each test score in the clinical population is provided in Table 1.

TABLE 1 The table describes the demographic and clinical characteristics of the patients with temporal lobe epilepsy, along with the scores of the neuropsychological tests.

Patients with TLE	Mean ± standard deviation
Age	46.73 ± 15.18
Age at onset	25.30 ± 19.55
Duration of epilepsy (years)	22.38 ± 20.46
TIQ	87.81 ± 19.74
TMT-A	34.45 ± 17.86
TMT-B	118.58 ± 73.77
Rey–Osterrieth Complex Figure	14.69 ± 6.47
Rey Auditory Verbal Learning Test	6.54 ± 2.93
Antiseizure medications	**Number**
CZP	1
ZNS	1
PB	1
OXC	2
ACT	2
LTG	3
None	3
BRV	4
LEV	6
VPA	6
CBZ	7
LAC	8
CLB	8
ESL	11
PER	11
MRI	**Number**
Mesial	9
HS	7
DNET	1
UKN	1
Anterior (temporal pole)	8
FCD	6
Encephalocele	1
Gliosis	1
Anterior + mesial	7
FCD + HS	7
Developmental venous anomaly	1
Supratentorial obstructive hydrocephalus	1
Negative MRI	11

Note: MRI abnormalities are reported by sublobar localization.

The continuous variables are reported as mean ± standard deviation.

Antiseizure Medication Abbreviations: ACT, acetazolamide; BRV, brivaracetam; CBZ, carbamazepine; CLB, clobazam; CZP, clonazepam; ESL, eslicarbazepine; LAC, lacosamide; LEV, levetiracetam; LTG, lamotrigine; NFT, no pharmacological treatment; OXB, oxcarbazepine; PB, phenobarbital; PER, perampanel; VPA, valproic acid; ZNS, zonisamide.

Abbreviation of the identified anomalies on the magnetic resonance imaging: DNET, dysembryoplastic neuroepithelial tumors; FCD, focal cortical dysplasia; HS, hippocampal sclerosis; UKN, unknown.

2.3 | Resting-state EEG recording

The hdEEG recordings were obtained using a 128-channel Micromed system referenced to the vertex. Data were sampled at 1024 Hz and the impedance was kept below 5 kΩ for each sensor. For each participant we recorded 10 min of closed-eyes RS while they were seated comfortably in a chair in a silent room.

2.4 | EEG preprocessing

Signal preprocessing was performed through EEGLAB 14.1.2b.[22] The continuous EEG signal was first downsampled at 256 Hz and then bandpass-filtered (0.1–45 Hz) using a Hamming windowed sinc finite impulse response filter. The signal was visually inspected to identify interictal epileptiform discharges (IEDs) by GMD, AD, and PB and then segmented into 2 s epochs. Epochs containing IED activity were successively removed. The epoched data were run through an automated cleaning algorithm using the TBT plugin implemented in EEGLAB (for the details please see Appendix S1). The previously mentioned preprocessing analysis pipeline has been applied by our group in previous studies investigating both task-related and RS EEG activity.[7,17] The data cleaning was performed using independent component analysis implemented via the Infomax algorithm in EEGLAB.[22] The resulting 40 independent components were visually inspected (both the topography and the time-series), and those related to eye blinks, eye movements, or muscle or cardiac artifacts were discarded. The remaining components were then back-projected to the electrode space. Finally, bad channels were reconstructed with the spherical spline interpolation method.[23] The data were then re-referenced to the average of all electrodes. At the end of the data preprocessing, each subject had at least 8 min of artifact-free signal.

2.5 | Cortical source modeling

We used the individual anatomy MRI to generate individualized head models for the patients with TLE. The anatomic MRI for source imaging consisted of a T1 1 mm isotropic three-dimensional (3D) acquisition (256 × 256 × 256 matrix). For three patients and for the control group we used the MNI-ICBM152 default anatomy[24] from Brainstorm,[25] since the 3D T1 MRI sequences were not available. The MRI was segmented in skin, skull, and gray matter using the Computational Anatomy Toolbox (CAT12) and then imported in Brainstorm, where we used Boundary Element Models (BEM) via OpenMEEG[26] to compute a realistic forward model (for the details please see Appendix S1). Finally, we used the weighted minimum norm estimation as the inverse model, with the default parameter settings provided in Brainstorm.

2.6 | Avalanche estimation

We extracted the activity of a total of 68 regions of interest (ROIs) from the Desikan-Killiany atlas.[27] The ROI time series was obtained by averaging the activity across the vertices composing each ROI. To study the dynamics of brain activity, we estimated "neuronal avalanches" from the source-reconstructed ROI time series. First, the time series of each ROI was binarized by calculating the z-score across time and then identifying positive and negative excursions beyond a threshold.

A neuronal avalanche begins when, in a sequence of contiguous time bins, at least one ROI is active (i.e. above the threshold of $|z\text{-score}| > 3$), and it ends when all ROIs are inactive.[10,28] Note that the ROIs are defined according to the parcellation of the MRI. Alternative z-score thresholds (i.e., 2.9 and 3.1) were tested. The total number of active ROIs in an avalanche corresponds to its size. These analyses require the time series to be binned. In fact, neuronal avalanches respond to specific properties that are derived from statistical mechanics, which are theoretically expected by a branching process operating near-critical regimen. Hence, the appropriate temporal binning allows capture of critical dynamics. To estimate the most reliable time bin length, for each subject, each neuronal avalanche, and each time bin duration, the branching parameter σ was estimated.[29] In fact, systems operating at criticality typically display a branching ratio ~1. The branching ratio is calculated as the geometrically averaged (over all the time bins) ratio of the number of events (activations) between the subsequent time bin (descendants) and that in the current time bin (ancestors) and then averaging it over all the avalanches.[30] More specifically:

$$\sigma_i = \prod_{j=1}^{N_{\text{bin}}-1} \cdot \left(\frac{n_{\text{events}}\,(j+1)}{n_{\text{events}}\,(j)} \right)^{\frac{1}{N_{\text{bin}}-1}} \tag{1}$$

$$\sigma = \prod_{i=1}^{N_{\text{aval}}} \cdot \left(\sigma_i\right)^{\frac{1}{N_{\text{aval}}}} \tag{2}$$

where σ_i is the branching parameter of the i_{th} avalanche in the data set, N_{bin} is the total amount of bins in the i_{th} avalanche, $n_{\text{events}}\,(j)$ is the total number of events active in the jth bin, and N_{aval} is the total number of avalanche in the data set. In our analyses the branching ratio was 1 for bin = 2 (8 ms).

2.7 | Transition matrices

Avalanches shorter than 2 time bins (~8 ms) were excluded from further analyses. However, the analyses were repeated also including only avalanches longer than 4 time bins (~16 ms), in order to focus on rare events (the sizes of the neuronal avalanches have a fat-tailed distribution) that are highly unlikely to be due to noise, and the results were unchanged[31] (see Figure S2). A matrix was calculated for each avalanche, where the elements in position (i, j) represented the probability that region j was active at time $t+\sigma$, given that region i was active at time t, where $\sigma \sim 8$ ms (see also Figure 1). The matrices were then averaged, edge-wise, across avalanches, as to obtain one avalanche transition matrix (ATM) per subject t. Then the ATMs were averaged, edge-wise, across subjects to obtain one matrix per group, and finally symmetrized. The introduction of a time lag makes it unlikely that our results can be explained trivially by volume conduction (i.e., the fact that multiple sources are detected simultaneously by multiple sensors, generating spurious zero-lag correlations in the recorded signals). Note that each edge is treated as an independent process. As such, if one region recruits more regions, this is captured by the presence of multiple edges in the transition matrix. For instance, for a binning of 2, as the avalanches proceed in time, the successive regions that are recruited do so after roughly 8 ms. Hence, activations occurring simultaneously do not contribute to the estimate of the ATM.

2.8 | Statistics

For each group, we computed the difference in the probability of a perturbation running across a given edge in patients and controls. To statistically validate the difference in the transition matrices across groups (patients with epilepsy vs control group), we randomly shuffled the labels of the ATMs across groups (i.e. each subject-specific transition matrix was randomly allocated to either the patients or the control group). We performed this procedure 10 000 times, obtaining, for each edge, the distribution of the differences given the null hypothesis that the ATMs would not capture any difference between the two groups. We used the null distribution to obtain a statistical significance for each edge. We applied false discovery rate (FDR) correction for multiple comparisons across edges.[32] Following this procedure, we obtained a matrix with the edges whose probabilities significantly differed between the two groups.

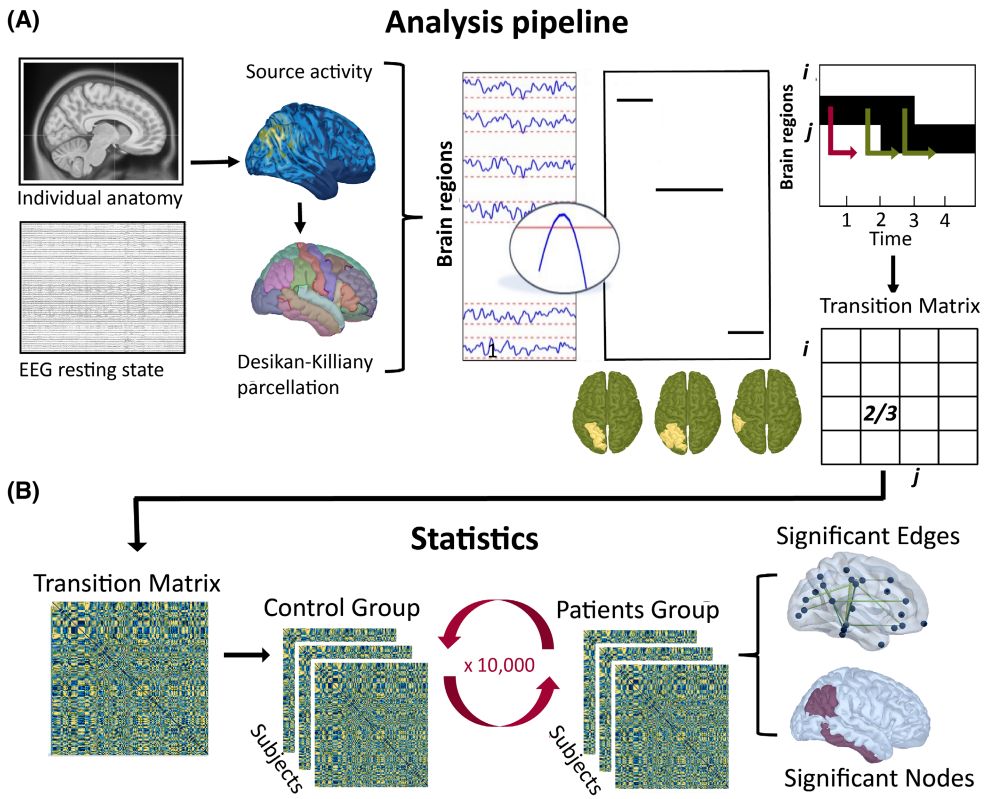

FIGURE 1 Graphical representation of analysis pipeline. The panel (A) of the figure represents the source reconstruction of the signal from resting-state EEG, and the following generation of the avalanche transition matrix after the source activity thresholding. Panel (B) illustrates the statistical procedure of the 10 000 permutation to extract significant edges and nodes.

Successively, we checked if the significantly different edges would cluster over specific brain regions. To this end, we computed the expected number of significant edges incident on any region, given a random distribution (with a comparable density), and selected those regions with an above-chance number of significant edges clustered upon them. Statistics were again corrected using FDR, this time across regions.

To check the consistency of the results we performed statistical analyses also for the z-score threshold of 2.9 and 3.1, and a different time binning including only avalanches longer than 4 time bins (16 ms).

2.8.1 | Correlations with the neuropsychological functioning

Finally, we investigated the relationship between the probability of an avalanche transition matrix and the neuropsychological functioning. At first, we extracted centrality measures for each node in the ATMs, namely, the eigenvector centrality, using the Brain Connectivity Toolbox.[33] Successively, we checked for the normality of data distribution using the Shapiro–Wilk test. We observed that the graph index was not normally distributed in the patients group ($p = .046$). For this reason, we applied Spearman's correlation between graph theory index of the statistically significant nodes and the neuropsychological measures. We then applied FDR correction across tests. Considering the relatively small sample size, in order to reduce the effect of the extreme value in the correlation computation, we applied winsorized robust correlations using the WRS2 package in R and Bayesian correlation with the software JASP. In this case we specifically targeted the significant results coming from the FDR-corrected correlation analysis. In addition, to control for potential effects related to the age we correlated the propagation index (PI) of the subjects, namely the mean across the non-zero elements of the ATMs, and the age of the two groups. In addition, we correlated the PI with the number of ASMs and the epilepsy duration. The age- and ASM-related correlations have been reported in the Appendix S1.

3 | RESULTS

We used the spatiotemporal spreading of large aperiodic bursts of activations as a proxy for communications between pairs of regions. Within this framework, large-scale, higher-order perturbations are considered to mediate the interactions between brain regions. We tested for differences between the two groups (i.e., patients with TLE and healthy controls) in the probabilities of any such perturbation propagating across two brain regions (avalanche transition matrix). The differences in the ATM were used to track (subject- and edge-wise) the difference on the spatial propagation of the perturbations across the two groups. To validate the observed differences, we built a null model randomizing the labels (i.e., patients or healthy control) 10 000 times, in order to obtain a null distribution of the differences expected by chance. These distributions were used to spot, individually, the edges that differed between the two conditions above chance level. We applied FDR to correct for multiple comparisons across edges.

As a first result we observed that the significant edges across groups were preferentially hinging the temporofrontal areas, suggesting that patients with TLE show increased transition probability in these areas (see Figure 2B; a list of the significant edges is present in the Appendix S1).

We then evaluated whether the significantly different edges would significantly cluster over specific brain regions. To this end, we computed the expected number of significant edges incident on any region, given a random network (with a comparable density as the observed ones), and selected those regions with an above-chance number of significantly different edges clustered upon them. Statistics were again corrected using FDR, this time across regions. These "reliably different" edges cluster preferentially upon the temporal and frontal regions. In particular, the left entorhinal cortex, the inferior parietal lobe, the left isthmus of the cingulate cortex, the right fusiform area, the right inferior and transversal temporal cortex, and the right rostral anterior cingulate cortex all showed to have significantly different edges clustered upon them ($p < .001$, FDR corrected).

These results were consistent across multiple z-score thresholds (2.9 and 3.1) as well as different time binnings (avalanche longer than 16 ms; see Figures S1 and S2).

Finally, we computed the eigenvector centrality (EC) in the ATM of each patient, and for the regions where different edges clustered, we related the individual EC to the neuropsychological scores. We observed a significant correlation ($r = -0.437$; $p_{adj} = .045$) between the EC of the left entorhinal cortex and the score of the delayed recall of the ROCFT in the group of patients with TLE. The results were robust to the outliers, as checked by the winsorized robust correlation ($r = -0.467$; $p = .013$). In addition, the Bayesian correlation revealed a Bayes factor in favor of the significant correlation ($r = -0.462$; $B_{10} = 4.706$).

To test the consistency of the results, we extended correlational analyses across multiple z-score thresholds (2.9 and 3.1) and avalanches longer than 4 time bins. We observed a significant correlation between the EC of the left entorhinal cortex and the score of the delayed recall of the

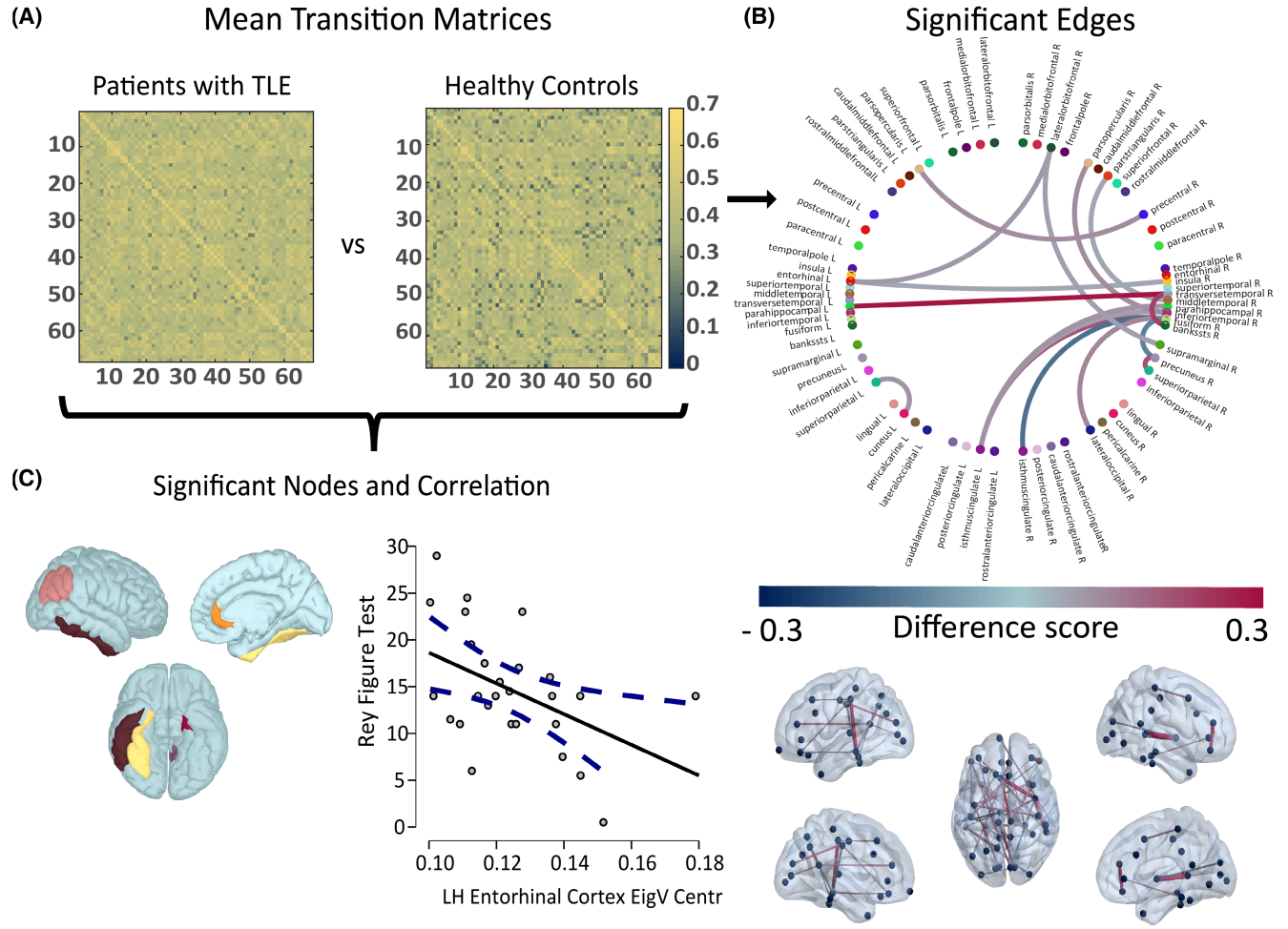

FIGURE 2 Results of the analyses. Panel (A) represents the group average of the avalanche transition probability matrices. Panel (B) (upper and lower parts) illustrates the significant edges differing between patients with temporal lobe epilepsy (TLE) and the control group. Finally, panel (C) indicates the significant nodes differing across groups, and the correlation of the left entorhinal cortex with the long-term memory performance (delay recall Rey–Osterrieth Complex Figure Test).

ROCFT (see Table S1). Moreover, it is worth mentioning that the direction of the correlation effect between the immediate recall of the verbal memory and the left entorhinal cortex centrality is close to statistical significance. This is in line with the relationship between the left temporal area and the verbal memory (see Appendix S1).

4 | DISCUSSION

In the present work we investigated the possible differences in the spontaneous, large-scale aperiodic activity occurring at rest in patients with TLE as compared to healthy controls.

We found that fast bursts of aperiodic activations ("neuronal avalanches") during RS are more likely to spontaneously spread across temporal areas in patients as compared to controls. We were able to provide such mapping starting from resting state, identifying areas that are typically involved in critical events in patients with TLE, and also display a (presumably) pathological role on the large-scale functional networks, regardless of the presence of epileptiform activity. By utilizing the avalanche transition matrices, that is, a mathematical tool that accommodates the non-linearities of the large-scale brain dynamics and the corresponding multimodal dynamics that they generate, we successfully identified the anomalous spreading of activity in patients with TLE from resting-state EEG data. The investigation of brain dynamics through the criticality framework represents a useful tool to describe the mechanisms underpinning the evolution of brain activity in terms of the aperiodic dynamics. However, criticality and neural avalanche have been applied mostly to identify epileptogenic areas[34] or characterizing brain dynamics during seizures.[15,16] It is important to note that our work is focused on the basal brain activity, assessing the intrinsic network organization of the brain with epilepsy when epileptiform activity is not occurring.

Although derived from the framework of criticality, the ATMs allowed us to move away from the traditional studies of the field, which focused only on the global properties of avalanches. In fact, we were able to evaluate the internal dynamics of avalanches, which may provide useful information on the specific brain regions involved in anomalous RS activity.

This line of thinking builds on converging evidence indicating that the brain alternates segregated and integrated states.[35,36] As such, meaningful communication among regions on a large scale would be intermittent and might be best understood and measured in terms of aperiodic perturbations. We reasoned that if avalanches convey interactions occurring between regions, then their spreading should also be modified between groups, if there is a different communicative basal pattern. Large-scale, in silico models have been used to investigate the generation and propagation of avalanches across the whole brain.[37] It was demonstrated that avalanches represent the large-scale correlate of groups of neuronal ensembles that become subsequently entrained by aperiodic perturbations. The ability of each region to respond or not to incoming stimuli depends on multiple factors, among which the structural connectome and the local properties are key elements. This reasoning from theoretical neurosciences provided us with the hypothesis that disrupted structural and/or functional properties, as seen in the regions typically involved in TLE, would also alter the ability of these regions to correctly receive, handle, and pass on stimuli originating from other parts of the brain. Our results identified in patients with TLE, in an unsupervised manner, a number of functional links (i.e. edges) across which avalanches are more likely to spread. The edges are mainly incident on temporal and frontocentral regions. These results align with the evidence of altered functional connectivity of temporal and frontal areas in TLE.[38,39] We observed that the significantly different edges hinged predominantly upon temporal regions such as the left entorhinal cortex and the fusiform area, as well as the superior temporal gyrus. These regions are known to be involved in TLE. In particular, the entorhinal cortex is considered a key player in seizure initiation in TLE.[40]

Furthermore, individuals with TLE frequently display altered functioning, often associated with a hyperactivation of the network involved in face recognition, including the fusiform area,[41,42] which we also find to be altered. Moreover, our results highlighted the involvement of the anterior cingulate cortex (ACC), which has been reported previously in TLE. In fact, evoked responses in the cingulate cortex have been detected after hippocampal stimulation in patients with TLE.[43] In addition, more recent evidence highlighted altered RS functional connectivity of the ACC in medial TLE.[44]

It is notable that the alterations in the avalanche spreading that we observed in TLE correlated with cognitive functioning. Specifically, we observed that the more the left entorhinal cortex was recruited by the transient bursts (i.e., higher centrality in the ATM), the worse were the cognitive performance in the long-term memory tasks (measured by the ROCFT).

The lateralization of this effect should not be interpreted, at the present stage, as a localization of the nonverbal memory in the left hemisphere. In fact, converging findings highlighted that, although being a reliable instrument for memory performance evaluation, the ROCFT is not sufficiently sensitive to characterize the lateralization of the memory functions.[45] This is probably related to the large network engagement related to the ROCFT, which to be performed involves also the left temporal lobe due to the verbalizability of many of its components.[46,47] In fact, previous findings highlighted that verbalization components partially compensate for the visuospatial deficit in the right TLE. It is important to note that the visuospatial deficit becomes evident as the task demands increase, and therefore represents an element to be investigated during the neuropsychological assessment.[48] However, there is strong evidence of nontrivial reliance on the left hippocampus in terms of resiliency of memory visuospatial functions after surgical resections, which warrants further investigation in terms of different effects of lateralization.[49] It is noteworthy that the ATM captures the whole-brain dynamics, including the contribution of the transition across a distributed network. Therefore, in relation to the limitations related to the lack of lateralization specificity of the ROCFT, the novelty of the present study, and our sample, we are only able to generate interpretative hypotheses in relation to the lateralization. In light of this, the correlation observed could be linked to the relationship between the recruitment of a distributed network from ROCFT and the whole-brain dynamics captured by ATMs. Additional investigations are necessary to better characterize the relationship between ATM and memory proficiency as a potential tool to shed light on neuronal mechanisms in left vs right TLE. However, due to our limited sample, it is not possible here to further discuss the lateralization of memory functions.

Nonetheless, our finding is particularly interesting, as it endows the spreading of activations in the data to a functional meaning, since it relates to a cognitive process that has been long known to be impaired in patients with TLE. In addition, it may be worth noting that the vast majority of large-scale brain-imaging studies have investigated the interactions among brain regions exploiting the statistical dependencies between the corresponding signals. With regard to epilepsy, one of the main focuses has been to characterize the behavior of brain networks during

seizures or IEDs, since they can provide the most relevant information in relation to diagnosis and also to treatment selection and planning. In contrast, here we exploited the spontaneous dynamics embedded in the simple raw signal, derived from source- activation maps of the resting activity, purposely disregarding epileptiform activity. It is striking that disregarding most of the signals and focusing on the aperiodic transients has allowed us to apply a remarkably simple pipeline, which avoids heavy filtering and assumptions of stationarity, and is applied in the time domain. In fact, by thresholding the *z*-scored signals, temporal regions naturally emerged as key players in the RS dynamics, beyond ictal or IED. However, it is important to note that we may have underestimated the true frequency of IEDs, since they may not be evident on surface EEG.

At the same time, it remains difficult to provide an unambiguous mechanistic interpretation of our findings. It might be that a potential alteration of the regional excitation/inhibition (E/I) balance could facilitate the recruitment of a given brain region by the ongoing transient large-scale perturbations. In the same line of thinking, Burrows et al.[50] observed that manipulating the E/I balance in cellular, in vivo neural networks caused a shift of the operational regimen away from criticality, which was linked, in turn, to the emergence of epileptic activity. Beyond the neuroscientific implications, our methodology might directly help the patients' management. In particular, the present methodology might serve as a non-invasive and cost-effective tool exploiting basal activity in order to identify specific profiles of functionally altered regions in different forms of epilepsy. Moreover, it can be used in complex diagnostic processes, such as those in which scalp EEG monitoring failed in recording seizure activity. In these scenarios, our methodology allows the identification of functionally altered zones that may be the target for additional investigation (e.g., intracranial recording). However, longitudinal studies are required to validate such findings in relation to clinical outcomes after surgical resection.

5 | CONCLUSIONS

Our study evaluated brain dynamics during RS activity in TLE as compared to healthy controls utilizing the framework of neuronal avalanches. We found specific alterations of the transition probability in the entorhinal cortex, the inferior temporal and fusiform gyri, and the anterior cingulate cortex. Higher eigenvector centrality (or EC) of the left entorhinal cortex was related to lower long-term memory performance. The present methodology might serve as a potential diagnostic tool identifying functionally altered regions, thereby aiding the diagnostic process.

AUTHOR CONTRIBUTIONS

Conceptualization: Gian Marco Duma and Pierpaolo Sorrentino. Methodology: Gian Marco Duma and Pierpaolo Sorrentino. Writing–original draft preparation: Gian Marco Duma, Pierpaolo Sorrentino, Alberto Danieli, Giovanni Mento, Viktor Jirsa, and Paolo Bonanni. Formal analysis: Gian Marco Duma and Pierpaolo Sorrentino. Data curation: Gian Marco Duma, Valerio Vitale, and Raffaella Scotto Opipari. Investigation: Gian Marco Duma, Pierpaolo Sorrentino, Alberto Danieli, Giovanni Mento, Viktor Jirsa, and Paolo Bonanni. Visualization: Gian Marco Duma and Pierpaolo Sorrentino. Supervision: Viktor Jirsa, Alberto Danieli, Paolo Bonanni, and Pierpaolo Sorrentino, Funding acquisition: Paolo Bonanni.

ACKNOWLEDGMENTS

This work was supported by a 2019 "5XMille" funds for biomedical research of The Italian Health Ministry to PB, by the European Union's Horizon 2020 research and 569 innovation program under grant agreement No. 945539 (SGA3) and by funds from the Italian Ministry of Health, Ricerca corrente 2023. Open access funding provided by BIBLIOSAN.

CONFLICT OF INTEREST STATEMENT

None of the authors has any conflict of interest to disclose. We confirm that we have read the Journal's position on issues involved in ethical publication and affirm that this report is consistent with those guidelines.

ORCID

Gian Marco Duma https://orcid.org/0000-0002-0778-3920
Viktor Jirsa https://orcid.org/0000-0002-8251-8860
Paolo Bonanni https://orcid.org/0000-0002-9448-9059
Pierpaolo Sorrentino https://orcid.org/0000-0002-9556-9800

REFERENCES

1. Zalesky A, Fornito A, Cocchi L, Gollo LL, Breakspear M. Time-resolved resting-state brain networks. Proc Natl Acad Sci USA. 2014;111(28):10341–6.
2. O'Byrne J, Jerbi K. How critical is brain criticality? Trends Neurosci. 2022;45:820–37.
3. Bartolomei F, Guye M, Wendling F. Abnormal binding and disruption in large scale networks involved in human partial seizures. EPJ Nonlinear Biomed Phys. 2013;1(1):1–16.
4. Bartolomei F, Lagarde S, Wendling F, McGonigal A, Jirsa V, Guye M, et al. Defining epileptogenic networks: contribution of SEEG and signal analysis. Epilepsia. 2017;58(7):1131–47.
5. Bernhardt BC, Bernasconi A, Liu M, Hong SJ, Caldairou B, Goubran M, et al. The spectrum of structural and functional imaging abnormalities in temporal lobe epilepsy. Ann Neurol. 2016;80(1):142–53.

6. Duma GM, Danieli A, Vettorel A, Antoniazzi L, Mento G, Bonanni P. Investigation of dynamic functional connectivity of the source reconstructed epileptiform discharges in focal epilepsy: a graph theory approach. Epilepsy Res. 2021;176:106745.
7. Duma GM, Di Bono MG, Mento G. Grounding adaptive cognitive control in the intrinsic, functional brain organization: an HD-EEG resting state investigation. Brain Sci. 2021;11(11):1513.
8. Fadaie F, Lee HM, Caldairou B, Gill RS, Sziklas V, Crane J, et al. Atypical functional connectome hierarchy impacts cognition in temporal lobe epilepsy. Epilepsia. 2021;62(11):2589–603.
9. Zimmern V. Why brain criticality is clinically relevant: a scoping review. Front Neural Circuits. 2020;14:54.
10. Shriki O, Alstott J, Carver F, Holroyd T, Henson RNA, Smith ML, et al. Neuronal avalanches in the resting MEG of the human brain. J Neurosci. 2013;33(16):7079–90.
11. Sorrentino P, Seguin C, Rucco R, Liparoti M, Lopez ET, Bonavita S, et al. The structural connectome constrains fast brain dynamics. Elife. 2021;10:e67400.
12. Sorrentino P, Rucco R, Baselice F, De Micco R, Tessitore A, Hillebrand A, et al. Flexible brain dynamics underpins complex behaviours as observed in Parkinson's disease. Sci Rep. 2021;11(1):4051. doi:10.1038/s41598-021-83425-4
13. Polverino A, Lopez ET, Minino R, Liparoti M, Romano A, Trojsi F, et al. Flexibility of fast brain dynamics and disease severity in amyotrophic lateral sclerosis. Neurology. 2022;99:e2395–405. https://doi.org/10.1212/WNL.0000000000201200
14. Arviv O, Medvedovsky M, Sheintuch L, Goldstein A, Shriki O. Deviations from critical dynamics in interictal epileptiform activity. J Neurosci. 2016;36(48):12276–92.
15. Meisel C, Storch A, Hallmeyer-Elgner S, Bullmore E, Gross T. Failure of adaptive self-organized criticality during epileptic seizure attacks. PLoS Comput Biol. 2012;8:e1002312. https://doi.org/10.1371/journal.pcbi.1002312
16. Osorio I, Frei MG, Sornette D, Milton J. Pharmaco-resistant seizures: self-triggering capacity, scale-free properties and predictability? Eur J Neurosci. 2009;30:1554–8. https://doi.org/10.1111/j.1460-9568.2009.06923.x
17. Duma GM, Danieli A, Mattar MG, Baggio M, Vettorel A, Bonanni P, et al. Resting state network dynamic reconfiguration and neuropsychological functioning in temporal lobe epilepsy: an HD-EEG investigation. Cortex. 2022;157:1–13.
18. Caffarra P, Vezzadini G, Dieci F, Zonato F, Venneri A. Rey-Osterrieth complex figure: normative values in an Italian population sample. Neurol Sci. 2002;22(6):443–7.
19. Carlesimo GA, Caltagirone C, Gainotti GUID, Fadda L, Gallassi R, Lorusso S, et al. The mental deterioration battery: normative data, diagnostic reliability and qualitative analyses of cognitive impairment. Eur Neurol. 1996;36(6):378–84.
20. Giovagnoli AR, Del Pesce M, Mascheroni S, Simoncelli M, Laiacona M, Capitani E. Trail making test: normative values from 287 normal adult controls. Ital J Neurol Sci. 1996;17(4):305–9.
21. Orsini A, Pezzuti L. WAIS-IV. Contribution to the Italian standardization. Giunti OS; 2013.
22. Delorme A, Makeig S. EEGLAB: an open source toolbox for analysis of single-trial EEG dynamics including independent component analysis. J Neurosci Methods. 2004;134(1):9–21.
23. Perrin F, Pernier J, Bertrand O, Echallier JF. Spherical splines for scalp potential and current density mapping. Electroencephalogr Clin Neurophysiol. 1989;72(2):184–7.
24. Evans AC, Janke AL, Collins DL, Baillet S. Brain templates and atlases. Neuroimage. 2012;62(2):911–22.
25. Tadel F, Baillet S, Mosher JC, Pantazis D, Leahy RM. Brainstorm: a user-friendly application for MEG/EEG analysis. Comput Intell Neurosci. 2011;2011:1–13.
26. Gramfort A, Papadopoulo T, Olivi E, Clerc M. OpenMEEG: opensource software for quasistatic bioelectromagnetics. Biomed Eng Online. 2010;9(1):1–20.
27. Desikan RS, Ségonne F, Fischl B, Quinn BT, Dickerson BC, Blacker D, et al. An automated labeling system for subdividing the human cerebral cortex on MRI scans into gyral based regions of interest. Neuroimage. 2006;31(3):968–80.
28. Beggs JM, Plenz D. Neuronal avalanches in neocortical circuits. J Neurosci. 2003;23(35):11167–77.
29. Haldeman C, Beggs JM. Critical branching captures activity in living neural networks and maximizes the number of metastable states. Phys Rev Lett. 2005;94(5):058101.
30. Bak P, Tang C, Wiesenfeld K. Self-organized criticality: an explanation of the 1/f noise. Phys Rev Lett. 1987;59(4):381–4.
31. Marshall N, Timme NM, Bennett N, Ripp M, Lautzenhiser E, Beggs JM. Analysis of power laws, shape collapses, and neural complexity: new techniques and MATLAB support via the NCC toolbox. Front Physiol. 2016;7:250.
32. Benjamini Y, Hochberg Y. Controlling the false discovery rate: a practical and powerful approach to multiple testing. J R Stat Soc Series B Stat Methodo. 1995;57(1):289–300.
33. Rubinov M, Sporns O. Complex network measures of brain connectivity: uses and interpretations. Neuroimage. 2010;52(3):1059–69.
34. Witton C, Sergeyev SV, Turitsyna EG, Furlong PL, Seri S, Brookes M, et al. Rogue bioelectrical waves in the brain: the Hurst exponent as a potential measure for presurgical mapping in epilepsy. J Neural Eng. 2019;16:56019. https://doi.org/10.1088/1741-2552/ab225e
35. Cohen JR, D'Esposito M. The segregation and integration of distinct brain networks and their relationship to cognition. J Neurosci. 2016;36(48):12083–94.
36. Fukushima M, Sporns O. Structural determinants of dynamic fluctuations between segregation and integration on the human connectome. Commun Biol. 2020;3(1):1–11.
37. Rabuffo G, Fousek J, Bernard C, Jirsa V. Neuronal cascades shape whole-brain functional dynamics at rest. ENeuro. 2021;8(5):1–9.
38. Maccotta L, He BJ, Snyder AZ, Eisenman LN, Benzinger TL, Ances BM, et al. Impaired and facilitated functional networks in temporal lobe epilepsy. NeuroImage Clin. 2013;2:862–72.
39. Qin L, Jiang W, Zheng J, Zhou X, Zhang Z, Liu J. Alterations functional connectivity in temporal lobe epilepsy and their relationships with cognitive function: a longitudinal resting-state fMRI study. Front Neurol. 2020;11:625.
40. Vismer MS, Forcelli PA, Skopin MD, Gale K, Koubeissi MZ. The piriform, perirhinal, and entorhinal cortex in seizure generation. Front Neural Circuits. 2015;9:27.
41. Guedj E, Bettus G, Barbeau EJ, Liégeois-Chauvel C, Confort-Gouny S, Bartolomei F, et al. Hyperactivation of parahippocampal region and fusiform gyrus associated with successful encoding in medial temporal lobe epilepsy. Epilepsia. 2011;52(6):1100–9.
42. Riley JD, Fling BW, Cramer SC, Lin JJ. Altered organization of face-processing networks in temporal lobe epilepsy. Epilepsia. 2015;56(5):762–71.

43. Kubota Y, Enatsu R, Gonzalez-Martinez J, Bulacio J, Mosher J, Burgess RC, et al. In vivo human hippocampal cingulate connectivity: a corticocortical evoked potentials (CCEPs) study. Clin Neurophysiol. 2013;124(8):1547–56.
44. Jo HJ, Kenney-Jung DL, Balzekas I, Welker KM, Jones DT, Croarkin PE, et al. Relationship between seizure frequency and functional abnormalities in limbic network of medial temporal lobe epilepsy. Front Neurol. 2019;10:488.
45. Wisniewski I, Wendling AS, Manning L, Steinhoff BJ. Visuospatial memory tests in right temporal lobe epilepsy foci: clinical validity. Epilepsy Behav. 2012;23(3):254–60.
46. Kneebone AC, Lee GP, Wade LT, Loring DW. Rey complex figure: figural and spatial memory before and after temporal lobectomy for intractable epilepsy. J Int Neuropsychol Soc. 2007;13(4):664–71.
47. Ono SE, de Carvalho Neto A, Joaquim MJM, Dos Santos GR, de Paola L, Silvado CES. Mesial temporal lobe epilepsy: revisiting the relation of hippocampal volumetry with memory deficits. Epilepsy Behav. 2019;100:106516.
48. Helmstaedter C, Pohl C, Elger CE. Relations between verbal and nonverbal memory performance: evidence of confounding effects Particulary in patients with right temporal lobe epilepsy. Cortex. 1995;31(2):345–55.
49. Chelune GJ. Hippocampal adequacy versus functional reserve: predicting memory functions following temporal lobectomy. Arch Clin Neuropsychol. 1995;10(5):413–32.
50. Burrows DR, Diana G, Pimpel B, Moeller F, Richardson MP, Bassett DS, et al. Single-cell networks reorganise to facilitate whole-brain supercritical dynamics during epileptic seizures. bioRxiv. 2021:2021.10.14.464473. https://doi.org/10.1101/2021.10.14.464473

SUPPORTING INFORMATION

Additional supporting information can be found online in the Supporting Information section at the end of this article.

How to cite this article: Duma GM, Danieli A, Mento G, Vitale V, Opipari RS, Jirsa V, et al. Altered spreading of neuronal avalanches in temporal lobe epilepsy relates to cognitive performance: A resting-state hdEEG study. Epilepsia. 2023;00:1–11. https://doi.org/10.1111/epi.17551